Real-time Imaging of an Experimental Intracranial Aneurysm in Rats

Haruka MIYATA,[1,2,3]* Kampei SHIMIZU,[1,4]* Hirokazu KOSEKI,[1,3,5]
Yu ABEKURA,[1,4] Hiroharu KATAOKA,[4] Susumu MIYAMOTO,[4]
Kazuhiko NOZAKI,[2] Shuh NARUMIYA,[6] and Tomohiro AOKI[1,3,6]

[1]Department of Molecular Pharmacology, Research Institute,
National Cerebral and Cardiovascular Center, Suita, Osaka, Japan;
[2]Department of Neurosurgery, Shiga University of Medical Science, Otsu, Shiga, Japan;
[3]Core Research for Evolutional Science and Technology (CREST) from Japan
Agency for Medical Research and Development (AMED), National Cerebral and
Cardiovascular Center, Suita, Osaka, Japan;
[4]Department of Neurosurgery, Kyoto University Graduate School of Medicine,
Kyoto, Kyoto, Japan;
[5]Department of Neurosurgery, Tokyo Women's Medical University
Medical Center East, Tokyo, Japan;
[6]Alliance Laboratory for Advanced Medical Research, Medical Innovation Center,
Kyoto University Graduate School of Medicine, Kyoto, Kyoto, Japan

Abstract

Subarachnoid hemorrhage due to rupture of a pre-existing intracranial aneurysm has quite a poor outcome in spite of intensive medical care. Hemodynamic stress loaded on intracranial arterial walls is considered as a trigger and a regulator of formation and progression of the disease, but how intracranial arterial walls or intracranial aneurysm walls behave under hemodynamic stress loading remains unclear. The purpose of this study was to visualize and analyze the wall motion of intracranial aneurysms to detect a pathological flow condition. We subjected a transgenic rat line, in which endothelial cells are specifically visualized by expression of a green fluorescent protein, to an intracranial aneurysm model and observed a real-time motion of intracranial arterial walls or intracranial aneurysm walls by a multiphoton laser confocal microscopy. The anterior cerebral artery–olfactory artery bifurcation was surgically exposed for the monitoring. First, we observed the proper flow-dependent physiological dilatation of a contralateral intracranial artery in response to increase of blood flow by one side of carotid ligation. Next, we observed intracranial aneurysm lesions induced in a rat model and confirmed that a wall motion of the dome was static, whereas that of the neck was more dynamic in response to pulsation of blood flow. We successfully monitored a real-time motion of intracranial aneurysm walls. Findings obtained from such a real-time imaging will provide us many insights especially about the correlation of mechanical force and the pathogenesis of the disease and greatly promote our understanding of the disease.

Key words: intracranial aneurysm, real-time imaging, bio-imaging, wall motion, rat

Introduction

Subarachnoid hemorrhage (SAH) due to rupture of a pre-existing intracranial aneurysm (IA) has quite

a poor outcome.[1] Thus, an appropriate treatment intervention to IAs as a preemptive one based on accurate understanding of their underlying pathogenesis is mandatory for social health.[2] Recent experimental studies and ones using human data or specimen have accumulated evidence regarding the pathogenesis and defined IAs as a macrophage-mediated chronic inflammatory disease affecting intracranial arterial walls.[3–8] In another point of view, hemodynamic stress loaded on intracranial arterial walls is considered as a trigger and a regulator of

*These authors equally contributed to this work.

formation and progression of the disease.[9–16)] Based on this assumption, it is a central question how hemodynamic stress is loaded on intracranial arterial walls, how it regulates inflammation in situ or what factor among various hemodynamic factors is important for the pathogenesis. However, how intracranial arterial walls or IA walls behave under hemodynamic stress loading remains unclear.

Currently, many believe that a hemodynamic force greatly influences the pathogenesis of an IA and thereby this disease is considered as a hemodynamics-sensitive one.[13,15,17)] Because such a concept is mainly developed through computational fluid dynamic (CFD) analysis of human cases or lesions induced in animal models, many remain to be elucidated mainly what indeed happens and what kind of molecular machineries drives in situ of an IA lesion loaded by a hemodynamic force. In imaging analysis, because of the limited spatiotemporal resolution of modalities used in a daily medical practice such as magnetic resonance angiography and computed tomography angiography, it is usually difficult to detect such a tiny and a rapid change of IA walls in response to remarkable changes in hemodynamic status due to heart beat. Furthermore, in humans, we can certainly monitor a motion of IA walls during surgery but this procedure needs the extensive resection of arachnoid bundles and dissection of connective tissues surrounding lesions presumably making results of imaging more artificial.

In this manuscript, to know better what happens in IA lesions in situ especially in response to hemodynamic stress loading and how hemodynamic force influences a morphology of IA lesions, we subjected a transgenic rat line, in which endothelial cells are specifically visualized by expression of a green fluorescent protein (GFP) to an IA model and observed real-time motion of IA walls by a multiphoton laser confocal microscopy.

Materials and Methods

Rodent IA models and histological analysis of induced IA

All of the following experiments, including animal care and use, complied with the National Institute of Health's Guide for the Care and Use of Laboratory Animals and were approved by the Institutional Animal Care and Use Committee of Kyoto University Graduate School of Medicine and also of National Cerebral and Cardiovascular Center.

Transgenic Wistar rat expressing GFP specifically in endothelial cells (W-Tg(Tek-GFP)1Soh[18)]) was supplied by the National BioResource Project-Rat at Kyoto University (Stock Number #0604, Kyoto, Japan, http://www.anim.med.kyoto-u.ac.jp/NBR/). Animals were maintained on a light/dark cycle of 14 h/10 h, and had a free access to chow and water. To induce IA, under general anesthesia by intraperitoneal injection of pentobarbital sodium (80 mg/kg), 7-week-old male rats (n = 9) were subjected to ligation of the left carotid artery and systemic hypertension induced by the combination of salt overloading and ligation of the left renal artery.[7,19,20)] Immediately after above surgical procedures, animals were fed the chow containing 8% sodium chloride and 0.12% 3-aminopropionitrile (Tokyo Chemical Industry, Tokyo, Japan), an inhibitor of lysyl oxidase that catalyzes the cross-linking of collagen and elastin, to exacerbate fragility of arterial walls and facilitate IA progression.[7,19,20)] At times indicated in the corresponding figure legends or results after aneurysm induction, animals were anesthetized by intraperitoneal injection with a pentobarbital sodium (80 mg/kg) and subjected to a real-time imaging experiment (n = 6) as shown in the next paragraph in detail. In some experiments, some animals were deeply anesthetized by intraperitoneal injection with a lethal dose of pentobarbital sodium, and transcardially perfused with 4% paraformaldehyde. The bifurcation site including the induced IA lesion concerned was then stripped, and serial frozen sections were made for immunohistochemistry.

Real-time imaging of intracranial arteries of rats

W-Tg(Tek-GFP)1Soh rats were subjected to a tracheotomy and a longitudinal split of mandible under general anesthesia (pentobarbital sodium, 80 mg/kg) (Fig. 1A), and performed a craniectomy of maxilla and skull base (Fig. 1B). An anterior cerebral artery (ACA)–olfactory artery (OA) bifurcation site of the circle of Willis located adjacent to an optic nerve was then exposed (Figs. 1C and 1D). Wall motion of arterial walls at this bifurcation site was visualized by expression of GFP in endothelial cells using a multiphoton-laser confocal microscopy system (A1MP, Nikon Corporation, Tokyo, Japan) and monitored. The frame rate of this imaging method was 30 frames/s. The excitation spectrum is 920 nm.

Immunohistochemistry

Immunohistochemical analyses were performed as previously described.[7,21)] Briefly, at the indicated period after aneurysm induction, 5-μm-thick frozen sections were prepared. After blocking with 3% donkey serum (Jackson ImmunoResearch, Baltimore, MD, USA), slices were incubated with primary antibodies followed
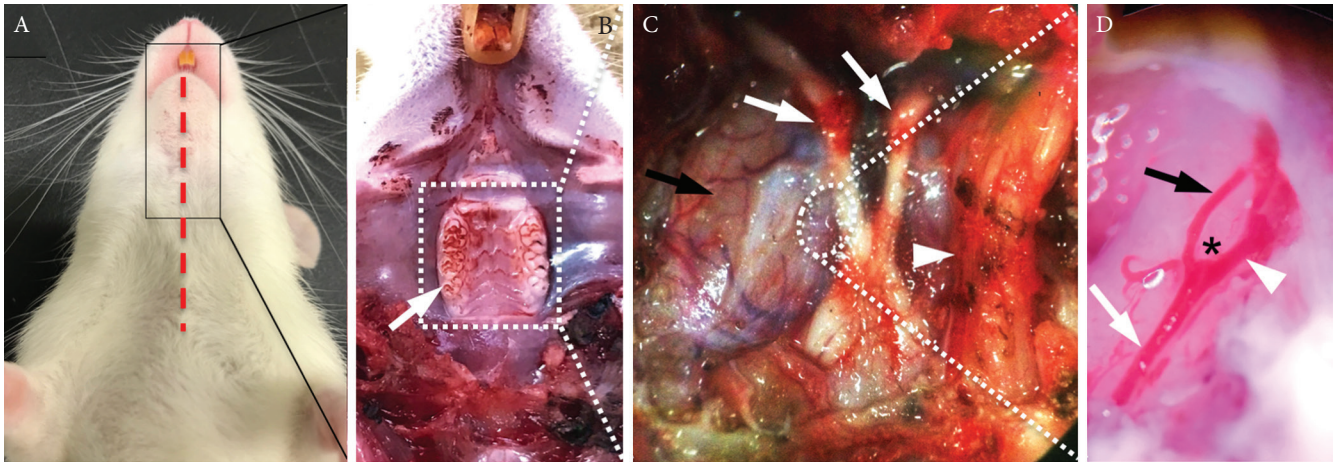
Fig. 1 The surgical exposure of an intracranial vasculature. (A–D) The surgical exposure of the anterior cerebral (ACA)–olfactory artery (OA) bifurcation site of the circle of Willis in a W-Tg(Tek-GFP)1Soh rat line. After the skin incision (*a red dash line* in A) and a longitudinal split of mandible, molars were exposed (a *white arrow* in B). Molars, maxilla and skull base were resected and a right trigeminal nerve was removed. Structures of skull base including bilateral optic nerves (*white arrows*), a left trigeminal nerve (a *white arrowhead*) and a surface of dura matter of right hemisphere (a *black arrow*) were then exposed (C). After the incision of dura (as shown in a *circle* in C), the ACA–OA bifurcation site with surrounding arteries was exposed (a *white arrow*; an internal carotid artery, a *white arrowhead*; ACA, *a black arrow*; OA, *asterisk*; a bifurcation site, D).

by incubation with secondary antibodies conjugated with a fluorescence dye (Jackson ImmunoResearch). Finally, fluorescent images were acquired on a confocal fluorescence microscope system (Lsm-710, Carl Zeiss Microscopy GmBH, Gottingen, Germany).

The following primary antibodies were used: anti-actin, α-smooth muscle-Cy3 antibody produced in mouse (#C6198, SIGMA, St. Louis, MO, USA), purified rat anti-mouse CD31 (#550274, BD Pharmingen, Franklin Lakes, NJ, USA).

Results

Endothelial cell-specific expression of GFP in a W-Tg(Tek-GFP)1Soh rat line

First, we examined expression of GFP in a W-Tg(Tek-GFP)1Soh rat line (Tie2-GFP transgenic rat line) to confirm a restricted expression in endothelial cells by immunohistochemistry. We harvested an intracranial artery as a sample and immunostained for GFP and, in some experiments, also for CD31 [Platelet endothelial cell adhesion molecule-1 (PECAM-1)], a marker for endothelial cells. We then found that GFP-positive cells were present in cells located at most lumen side of intracranial arteries (Fig. 2A) and these cells were positive also for CD31 (Fig. 2A), confirming endothelial cell-specific expression of GFP in a W-Tg(Tek-GFP)1Soh rat line. Furthermore, in common carotid artery and thoracic aorta of this rat line, we validated that GFP-positive cells were also positive for CD31 and

thus GFP expression was restricted in endothelial cells as well (Figs. 2B and 2C).

Flow-dependent dilatation of intracranial arteries in response to unilateral ligation of the common carotid artery

It is well known that a vasculature dilates (increases radius) in response to increase of blood flow to maintain a wall shear stress (WSS) loaded within a certain range based on Poiseuille equation. Thereby, to verify that our observation obtained from a real-time imaging technique of intracranial arteries in this study indeed reflects a normal physiological response, we ligated a unilateral cervical common carotid artery (left) and monitored a change in a diameter of an arterial wall of a contralateral (right) internal carotid artery. The diameter of a right intracranial internal carotid artery before the ligation of a left cervical common carotid artery was 135 μm (Fig. 3A) whereas the diameter after ligation was 177 μm (Fig. 3B). Therefore, as expected, we could detect the physiological dilatation of an internal carotid artery in response to an increase of blood flow (Fig. 3C).

Real-time imaging of IA walls in a rat model

Rats were subjected to aneurysm induction and an IA lesion at the ACA–OA bifurcation was surgically exposed at 8 weeks after induction. Three rats among six rats surgically manipulated developed IAs at the ACA–OA bifurcation. We then monitored
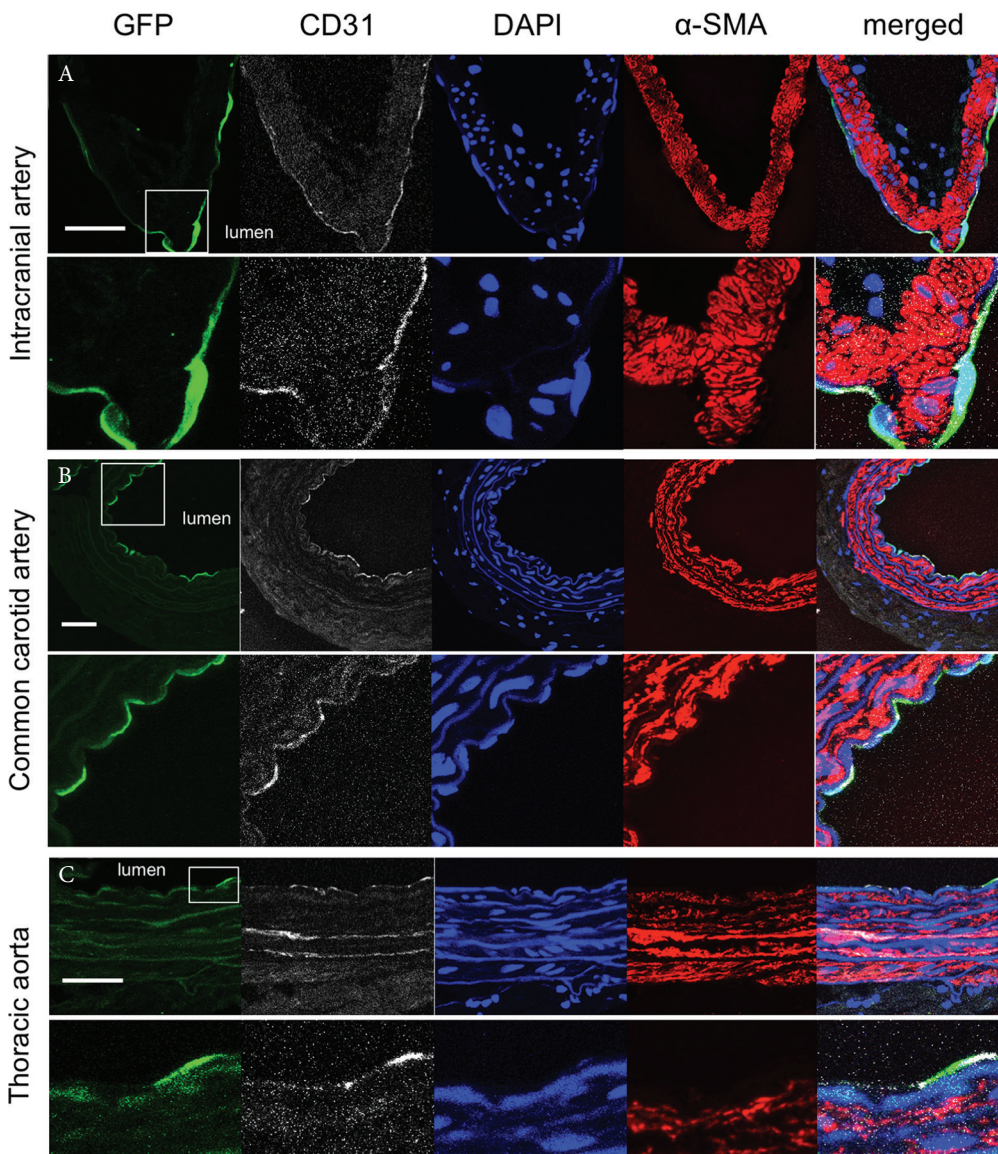
Fig. 2 Endothelial cell-specific expression of GFP in a W-Tg(Tek-GFP)1Soh (Tie2-GFP) rat line. Representative images of immunostaining of specimens from a cerebral artery (A), a common carotid artery (B) or a thoracic aorta (C) for GFP (*green*), CD31 (*white*), a marker of endothelial cells, α-smooth muscle actin (α-SMA, *red*), a marker of vascular smooth muscle cells, nuclear staining by DAPI (*blue*) and merged images are shown. In lower panels, magnified images corresponding to a *white square* in upper panels are shown. Bar: 20 µm.
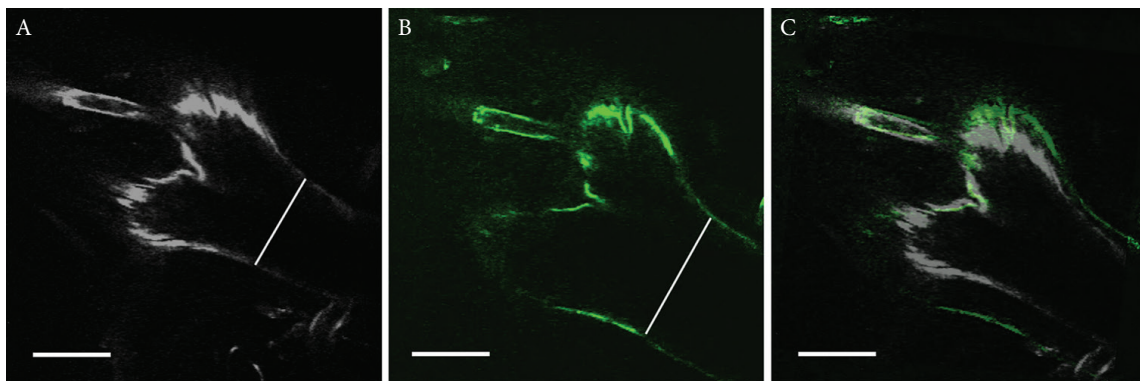

Fig. 3 A physiological flow-dependent dilatation of intracranial arteries in response to ligation of the contralateral cervical common carotid artery. Freeze-frames of a right ACA–OA bifurcation site and surrounding arterial walls obtained from a real-time imaging before (A) or 4 h after (B) the ligation of left cervical common carotid artery. The overlaid image of A and B is shown in C. Noted the dilatation of right intracranial internal carotid artery after the ligation of a left common carotid artery (as shown by a *white line* in each image, 135 µm in A, 177 µm in B). Bar: 100 µm.

a spatiotemporal movement of the IA lesion with surrounding arterial walls at the ACA–OA bifurcation site (30 frames/s, Fig. 4A). We traced out the wall of the ACA–OA bifurcation including the IA wall induced there through referencing expression of GFP in endothelial cells on sequentially acquired images (Fig. 4B). By comparing the traced line at each time point, we found that a motion of the neck was more dynamic than that of the dome (Figs. 4C and 4D).

Discussion

The real-time imaging demonstrated here revealed the heterogeneous wall motion in IA lesions induced at ACA–OA bifurcation of a rat model, indicating that the wall motion can be mechanical stimuli to cellular components in each part of arterial walls and may influence a biological process in microenvironment there leading to IAs. The major mechanical force loaded on arterial walls by blood flow and its pulsation are tensile stress and WSS.[22] Our observation from a real-time live imaging of IAs induced in a rat model that at the neck portion wall motion is dynamic during cardia cycle but almost a kinetic at the dome may be consistent with previous studies by a numerical simulation. In a numerical simulation, both tensile stress and WSS are highest at the neck portion but are remarkable low at the dome except for blebs.[9,10,12,13] Here, strength of tensile stress is tens of times higher than that of WSS.[23] Furthermore, it is of note that, in many CFD analyses, wall properties are assumed to be an isotropic non-linear hyperelastic or linear
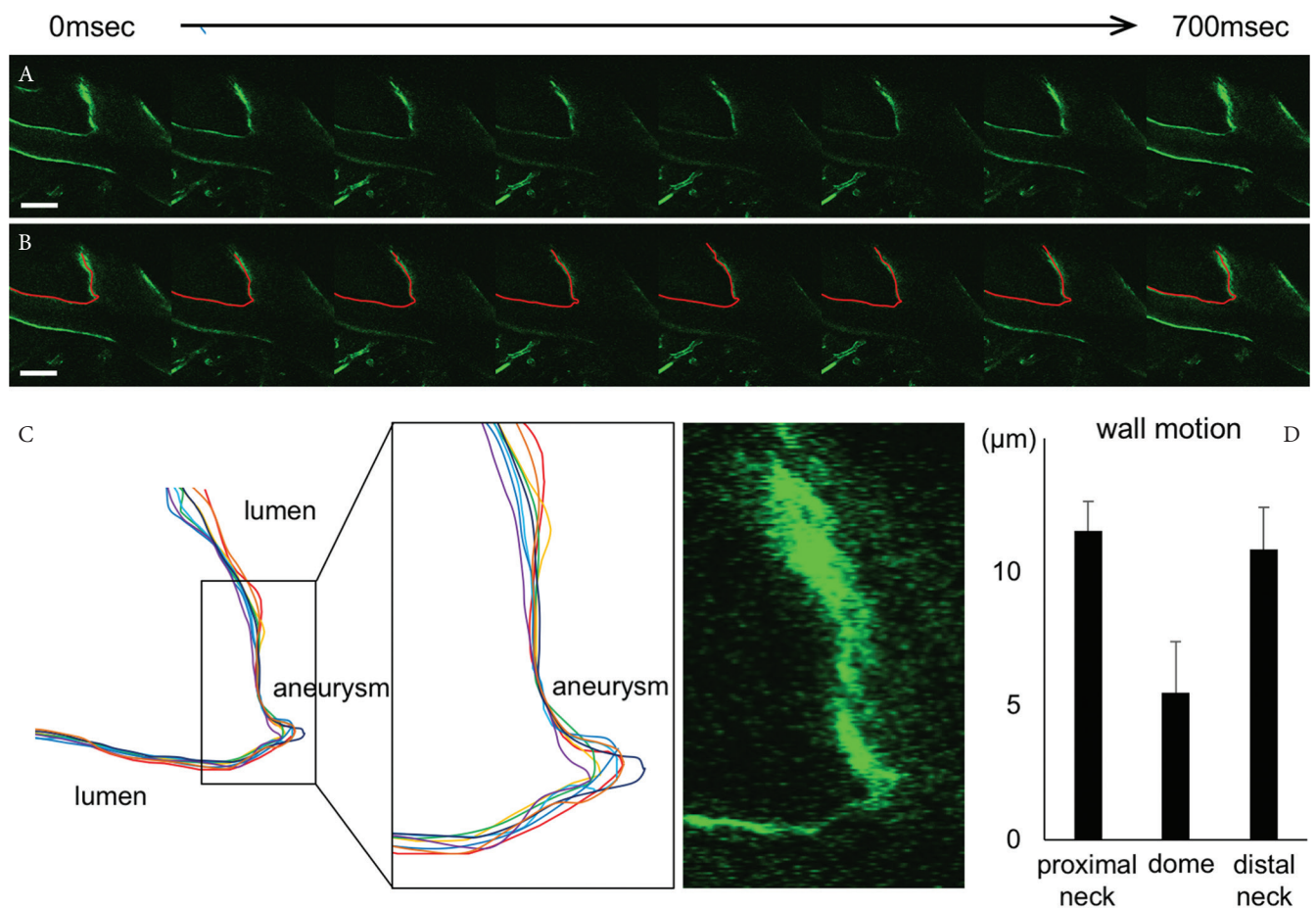
Fig. 4 **Real-time imaging of IA lesions in a rat model. (A and B), Serial freeze-frame images from a real-time imaging analysis by a multiphoton-laser confocal microscopy system. The IA lesion induced at the ACA–OA bifurcation site of W-Tg(Tek-GFP)1Soh (Tie2-GFP) rat at 8 weeks after aneurysm induction was monitored. Serial freeze-frame images at about every 100 ms were obtained (A) and traced out by a *red line* (B). Representative images from one out of 3 rats were investigated. (C) The overlaid images of each traced line at each time point. Magnified images corresponding to the *square* in the left panel and a fluorescent image of GFP expressed in endothelial cells obtained from a real-time imaging are also shown. (D) Maximum displacement of the dome, the proximal neck and the distal neck. All bars represent mean ± SEM (*n* = 3).**

elastic material, and wall thickness to be uniform of 30–300 μm.[23,24] It thus remains unclear whether WSS can indeed distort arterial walls. Meanwhile, in addition of a direct mechanical impact, non-physiological WSS loaded on prospective site of IA formation or IA walls may influence the wall motion by affecting a wall property (i.e. elasticity). For example, in a rabbit model of IAs, high WSS and positive WSS gradient correlates with the histological changes resembling IAs, i.e. degeneration and thinning of arterial walls,[25,26] presumably through induction of matrix metalloproteinase-9 (MMP-9)[27] and reduction in the stiffness. Also, decreased expression of endothelial nitric oxide synthase is observed resulting in the maladaptation to increase of WSS.[28] Furthermore, in in vitro experiment, non-physiological excessive low WSS observed in the dome induces expression of chemoattractants for macrophages like monocyte chemoattractant protein-1 in cultured endothelial cells and presumably facilitate degeneration of arterial walls in situ through macrophage-producing MMP-9.[9]

In the present study, we used an already-established transgenic rat line[18] supplied by the National BioResource Project-Rat at Kyoto University. This rat line has been established in Wistar rat but unfortunately in this line the size of aneurysms induced at ACA–OA bifurcation is remarkably smaller than that in SD rat which we have usually used.[3,7,27] We have thus been trying to establish a similar rat line in which a fluorescent protein is expressed specifically in endothelial cell to make a real-time imaging more precisely reflecting human IAs. In addition to transgenic rat lines, recently, establishment of a gene-deficient rat line or other type of a gene-modified line becomes much easier thanks to development of the CRISPR/Cas9 system[29] or some other genome-editing techniques. Thereby, we can establish various rat lines necessary for examinations to clarify machineries regulating IA pathogenesis, i.e. for visualization of a certain cell type, of expression of some objective factors or of activation of signaling molecules. We and others have clarified the involvement of chronic inflammatory responses in intracranial arterial walls presumably triggered by high WSS in the pathogenesis of IAs[7,15,17,19,30,31] but the precise causative relationship between hemodynamic force and induction of pro-inflammatory factors remains to be elucidated because of the lack of methods to simultaneously examine mechanical force and molecular events. A real-time monitoring of intracranial arteries in a gene-modified rat line during IA development will thus greatly promote our understanding of the pathogenesis.

One of the major limitations in this experiment is a relatively low frame rate, 30 frames/s. Because a heart rate of a rat is several times higher than that in human, about 300–400 beats/min (over 5 beats/s), 30 frames/s is not adequate to monitor many important events in situ such as a streamline and a flow-dependent motion of monocytes. Equipment of high-speed CCD camera will thus be certain to provide us many important insights about flow-dependent events in situ.

Conclusion

In this study, we demonstrated a real-time imaging of IA lesions induced in a rat model and found that a wall motion is not uniform but rather remarkably different even within one IA lesion. Because hemodynamic force greatly influences the pathogenesis of IAs, the precise understanding of the pathological hemodynamic condition is essential to get a whole picture of IA development. In addition, a causative relationship between such a hemodynamic force and molecular events leading to IA development should be clarified to identify the pathological hemodynamic condition and responsible biological process. In a rat model, we have indeed examined molecular events happening in situ during IA development and revealed some important machineries, like a macrophage-mediated chronic inflammation, contributing to the pathogenesis. Establishment of a real-time imaging technique described in this manuscript will thus greatly help our understanding of the pathogenesis and contribute to develop a novel diagnostic strategy such as a detection of a pathological hemodynamic force as a marker of rupture-prone lesions and a novel therapeutic drug to prevent rupture of IAs.

Acknowledgments

Conflicts of Interest Disclosure

References

1) van Gijn J, Kerr RS, Rinkel GJ: Subarachnoid haemorrhage. *Lancet* 369: 306–318, 2007

2) Aoki T, Nozaki K: Preemptive medicine for cerebral aneurysms. *Neurol Med Chir* (*Tokyo*) 56: 552–568, 2016

3) Aoki T, Kataoka H, Ishibashi R, Nozaki K, Egashira K, Hashimoto N: Impact of monocyte chemoattractant protein-1 deficiency on cerebral aneurysm formation. *Stroke* 40: 942–951, 2009

4) Kanematsu Y, Kanematsu M, Kurihara C, et al.: Critical roles of macrophages in the formation of intracranial aneurysm. *Stroke* 42: 173–178, 2011

5) Frösen J, Tulamo R, Paetau A, et al.: Saccular intracranial aneurysm: pathology and mechanisms. *Acta Neuropathol* 123: 773–786, 2012

6) Aoki T, Narumiya S: Prostaglandins and chronic inflammation. *Trends Pharmacol Sci* 33: 304–311, 2012

7) Aoki T, Frösen J, Fukuda M, et al.: Prostaglandin E2-EP2-NF-κB signaling in macrophages as a potential therapeutic target for intracranial aneurysms. *Sci Signal* 10: 465, eaah6037 2017

8) Aoki T, Yamamoto R, Narumiya S: Targeting macrophages to treat intracranial aneurysm. *Oncotarget* 8: 104704–104705, 2017

9) Aoki T, Yamamoto K, Fukuda M, Shimogonya Y, Fukuda S, Narumiya S: Sustained expression of MCP-1 by low wall shear stress loading concomitant with turbulent flow on endothelial cells of intracranial aneurysm. *Acta Neuropathol Commun* 4: 48, 2016

10) Takeuchi S, Karino T: Flow patterns and distributions of fluid velocity and wall shear stress in the human internal carotid and middle cerebral arteries. *World Neurosurg* 73: 174–185; discussion e27, 2010

11) Boussel L, Rayz V, McCulloch C, et al.: Aneurysm growth occurs at region of low wall shear stress: patient-specific correlation of hemodynamics and growth in a longitudinal study. *Stroke* 39: 2997–3002, 2008

12) Tanoue T, Tateshima S, Villablanca JP, Viñuela F, Tanishita K: Wall shear stress distribution inside growing cerebral aneurysm. *AJNR Am J Neuroradiol* 32: 1732–1737, 2011

13) Dolan JM, Kolega J, Meng H: High wall shear stress and spatial gradients in vascular pathology: a review. *Ann Biomed Eng* 41: 1411–1427, 2013

14) Shojima M, Oshima M, Takagi K, et al.: Magnitude and role of wall shear stress on cerebral aneurysm: computational fluid dynamic study of 20 middle cerebral artery aneurysms. *Stroke* 35: 2500–2505, 2004

15) Turjman AS, Turjman F, Edelman ER: Role of fluid dynamics and inflammation in intracranial aneurysm formation. *Circulation* 129: 373–382, 2014

16) Can A, Du R: Association of hemodynamic factors with intracranial aneurysm formation and rupture: systematic review and meta-analysis. *Neurosurgery* 78: 510–520, 2016

17) Fukuda M, Aoki T: Molecular basis for intracranial aneurysm formation. *Acta Neurochir Suppl* 120: 13–15, 2015

18) Ohtsuki S, Kamiya N, Hori S, Terasaki T: Vascular endothelium-selective gene induction by Tie2 promoter/enhancer in the brain and retina of a transgenic rat. *Pharm Res* 22: 852–857, 2005

19) Aoki T, Nishimura M, Matsuoka T, et al.: PGE(2)-EP(2) signalling in endothelium is activated by haemodynamic stress and induces cerebral aneurysm through an amplifying loop via Nf-κB. *Br J Pharmacol* 163: 1237–1249, 2011

20) Hashimoto N, Handa H, Hazama F: Experimentally induced cerebral aneurysms in rats. *Surg Neurol* 10: 3–8, 1978

21) Miyata H, Koseki H, Takizawa K, et al.: T cell function is dispensable for intracranial aneurysm formation and progression. *PloS ONE* 12: e0175421, 2017

22) Ando J, Yamamoto K: Effects of shear stress and stretch on endothelial function. *Antioxid Redox Signal* 15: 1389–1403, 2011

23) Torii R, Oshima M, Kobayashi T, Takagi K, Tezduyar TE: Fluid–structure interaction modeling of aneurysmal conditions with high and normal blood pressures. *Comput Mech* 38: 482–490, 2006

24) Isaksen JG, Bazilevs Y, Kvamsdal T, et al.: Determination of wall tension in cerebral artery aneurysms by numerical simulation. *Stroke* 39: 3172–3178, 2008

25) Metaxa E, Tremmel M, Natarajan SK, et al.: Characterization of critical hemodynamics contributing to aneurysmal remodeling at the basilar terminus in a rabbit model. *Stroke* 41: 1774–1782, 2010

26) Meng H, Wang Z, Hoi Y, et al.: Complex hemodynamics at the apex of an arterial bifurcation induces vascular remodeling resembling cerebral aneurysm initiation. *Stroke* 38: 1924–1931, 2007

27) Aoki T, Kataoka H, Morimoto M, Nozaki K, Hashimoto N: Macrophage-derived matrix metalloproteinase-2 and -9 promote the progression of cerebral aneurysms in rats. *Stroke* 38: 162–169, 2007

28) Wang Z, Kolega J, Hoi Y, et al.: Molecular alterations associated with aneurysmal remodeling are localized in the high hemodynamic stress region of a created carotid bifurcation. *Neurosurgery* 65: 169–177; discussion 177–178, 2009

29) Doudna JA, Charpentier E: Genome editing. The new frontier of genome engineering with CRISPR-Cas9. *Science* 346: 1258096, 2014

30) Aoki T, Nishimura M: Targeting chronic inflammation in cerebral aneurysms: focusing on NF-kappaB as a putative target of medical therapy. *Expert Opin Ther Targets* 14: 265–273, 2010

31) Aoki T, Kataoka H, Shimamura M, et al.: NF-kappaB is a key mediator of cerebral aneurysm formation. *Circulation* 116: 2830–2840, 2007

Address reprint requests to: Tomohiro Aoki, Department of Molecular Pharmacology, Research Institute, National Cerebral and Cardiovascular Center, 5-7-1 Fujishiro-dai, Suita, Osaka 565-8565, Japan.
e-mail: tomoaoki@ncvc.go.jp